

1

2 **Structural basis of the Sec translocon and YidC revealed through X-ray crystallography**

3

4

Tomoya Tsukazaki*

5

6

Nara Institute of Science and Technology, Ikoma, Nara 630-0192, Japan

7

8

9

10 *Correspondence should be addressed to T.T. (tsukazaki@mac.com)

11 Abstract

12 Protein translocation and membrane integration are fundamental, conserved processes. After or during
13 ribosomal protein synthesis, precursor proteins containing an N-terminal signal sequence are directed to a
14 conserved membrane protein complex called the Sec translocon (also known as the Sec translocase) in the
15 endoplasmic reticulum membrane in eukaryotic cells, or the cytoplasmic membrane in bacteria. The Sec
16 translocon comprises the Sec61 complex in eukaryotic cells, or the SecY complex in bacteria, and mediates
17 translocation of substrate proteins across/into the membrane. Several membrane proteins are associated with
18 the Sec translocon. In *Escherichia coli*, the membrane protein YidC functions not only as a chaperone for
19 membrane protein biogenesis along with the Sec translocon, but also as an independent membrane protein
20 insertase. To understand the molecular mechanism underlying these dynamic processes at the membrane,
21 high-resolution structural models of these proteins are needed. This review focuses on X-ray crystallographic
22 analyses of the Sec translocon and YidC and discusses the structural basis for protein translocation and
23 integration.

24

25 Key words

26 protein translocation

27 protein insertion

28 X-ray crystallography

29 membrane protein

30 Sec translocon

31

32 **Introduction**

33 Membrane or secretory proteins are synthesized by cytoplasmic ribosomes, and their nascent
34 polypeptides possess a specific membrane-targeted signal sequence for transport across or integration into the
35 membrane. The transported polypeptides then fold into mature proteins and function at the appropriate
36 locations. The membrane restricts the passive diffusion of small molecules and ions across the membrane. To
37 overcome the membrane permeability barrier and environmental factors such as the pH or salt concentration,
38 sophisticated machineries present in the membrane enable protein translocation across and integration into
39 the membrane. The Sec translocon is an evolutionarily conserved protein-conducting channel at the
40 endoplasmic reticulum (ER) membrane of eukaryotic cells, or the cytoplasmic membrane of bacteria and
41 archaea (Fig. 1A)^{1,2}. The Sec translocon is an essential hetero-ternary protein complex, comprising membrane
42 proteins Sec61 $\alpha/\gamma/\beta$ in eukaryotic cells or SecY/E/G in bacteria (Fig. 1B), and is involved in translocation and
43 integration of nascent ribosomally synthesized, unfolded proteins, in a signal sequence-dependent manner. In
44 the case of soluble proteins, the N-terminal membrane-targeting signal sequences of precursor proteins are
45 cleaved during translocation, thus decreasing the size of the mature proteins³. In many membrane proteins,
46 the first transmembrane region contains the targeting signal and is not cleaved. As shown in Figure 1, protein
47 translocation via the Sec translocon is classified into co-translational and post-translational translocations.
48 The basic mechanism of co-translational translocation in bacteria and eukaryotic cells is the same. During
49 co-translational translocation, the highly hydrophobic signal sequence emerging from the ribosomal exit
50 tunnel is recognized by the signal-recognition particle (SRP) and is targeted to the membrane
51 co-translationally, along with the ribosome, owing to interactions between the SRP and the SRP receptor
52 present in the membrane⁴. Thereafter, the ribosome directly interacts with the protein-conducting channel (i.e.,
53 the Sec translocon), which is present in the membrane. Subsequently, protein translocation occurs
54 simultaneously with protein translation. During post-translational translocation, unfolded proteins are targeted
55 to the membranes. The Sec62/63 complex and BiP protein are involved in this translocation in eukaryotic
56 cells. BiP proteins drive protein translocation via a ratchet mechanism, which can move in only one direction
57 owing to substrate interactions and conformational transitions of BiP by ATP hydrolysis⁵. In *Escherichia coli*,

58 precursor proteins, maintained in an unfolded state by chaperones such as SecB, are directed to the membrane
59 where the SecA ATPase drives protein translocation^{6,7}, although many chaperones including SecB are not
60 essential for the viability of *E. coli*. SecA repeatedly undergoes conformational changes to move the precursor
61 protein into the Sec translocon, using energy from ATP hydrolysis⁸. Because the Sec translocon itself is a
62 passive protein channel, other factors, including Sec62/63, SecA, and BiP, play indispensable roles in protein
63 translocation, as described above. Data from an electron microscopy study demonstrated that the eukaryotic
64 Sec translocon is associated with translocon-associated proteins (TRAPs) and the oligosaccharyl-transferase
65 (OST)^{9,10}. The cryo-electron microscopic density map of a TRAP showed it protruding into the ER space,
66 probably interacting with the substrate protein during protein translocation. In bacteria and archaea, the
67 SecD–SecF complex (SecDF), which interacts with Sec YEG, promotes protein translocation^{11,12}. SecDF
68 repeatedly undergoes drastic conformational changes with the substrate at the trans side of the plasma
69 membrane using proton motive force, which promotes substrate release into the trans-side space¹³⁻¹⁵. SecDF
70 can drive protein translocation at the trans side of the plasma membrane independently of SecA¹³. Hence,
71 SecDF is considered a second protein-translocation motor. The bacterial Sec translocon is involved in
72 membrane protein sorting during co-translational translocation in collaboration with YidC, a membrane
73 protein^{16,17}. YidC functions as a chaperone, facilitating co-translational membrane protein folding. Moreover,
74 YidC directly binds to the ribosome and is responsible for membrane insertion of certain single- and
75 double-spanning membrane proteins. Additionally, MPIase (membrane protein integrase), a glycolipozyme,
76 also plays an essential role in membrane protein insertion, before YidC inserts proteins into the membrane^{18,19}.
77 YidC corresponds to plant Alb3 in the thylakoid membrane and eukaryote Oxa1 in the inner mitochondrial
78 membrane (Fig. 1C). The YidC/Oxa1/Alb3 family proteins, containing five conserved transmembrane
79 α -helices, are involved in membrane protein insertion and assembly of the respiratory chain-related complex²⁰.
80 YidC of gram-negative bacteria possesses additional transmembrane and periplasmic regions (P1) at its
81 N-terminus. This review is focused on studies of the crystal structures of the Sec translocon and YidC, aimed
82 at elucidating the mechanisms underlying protein transport across/into the membrane at the atomic level, and
83 provides a detailed and comprehensive description of these membrane proteins.

84

85 **Architecture of Sec translocon**

86 Molecular modeling based on the first reported crystal structure of the Sec translocon in 2004 (Fig.
87 2A left, B)²¹ provided many insights into the mechanisms of protein translocation across and integration into
88 the membrane, via the Sec translocon. Subsequently, different types of functional analyses were performed to
89 elucidate the molecular mechanism underlying the action of Sec translocon^{1,2,22}. The available crystal
90 structure models of Sec translocons in the Protein Data Bank (PDB)^{21,23-28} are summarized in Table 1. The
91 first reported structure of the Sec translocon is from an archaeon, *Methanocaldococcus jannaschii*²¹, and is
92 designated as SecYE β in this review. As of March 20, 2019, the highest-resolution structure of the Sec
93 translocon was reported in 2014 for *Thermus thermophilus* SecYEG (2.7-Å resolution; Fig. 2A, right)²⁷.
94 Some reports do not include SecG/ β , a non-essential subunit²⁹⁻³², because it easily dissociates from the
95 essential SecYE complex and does not influence its stability. Purified *T. thermophilus* SecYEG, generated by
96 overexpressing SecG with an additional plasmid in SecYEG-overexpressing cells, was crystallized in the
97 lipidic cubic phase, facilitating determination of a high-resolution structure of the Sec translocon²⁷. Both the
98 *M. jannaschii* SecYE β and *T. thermophilus* SecYEG crystal structures represent the resting states of the Sec
99 translocon (Fig. 2A, B). Ten transmembrane α -helices of SecY compose the core of the Sec translocon, which
100 is stabilized by the cytoplasmic α -helix parallel to the membrane and the tilted transmembrane α -helix of
101 single-membrane-spanning SecE (triple membrane-spanning, in the case of *E. coli*). SecG, containing two
102 transmembrane α -helices, is peripherally located adjacent to transmembrane region 1 (TM1) and TM4 of
103 SecY. The single-membrane-spanning protein, Sec β , an alternative component of SecG, is located in a
104 position similar to that of SecG. The N-terminal and C-terminal halves, TM1–5 and TM6–10, respectively,
105 are arranged in a pseudosymmetrical manner and linked by a cytoplasmic loop, called a hinge. The protruding
106 cytoplasmic region 4 (C4) between the TM6–7 regions and C5 between the TM8–9 regions provide major
107 interaction sites for cytosolic factors, including SecA and ribosomes. The interior channel of SecY is
108 hourglass-shaped, its center containing a constricted region called the pore ring (Fig. 2C). The narrow point is
109 formed by six hydrophobic amino acid residues, primarily including Ile, at the middle regions of TM2, 5, 7,

110 and 10, and does not permit secretion of substrate proteins via the Sec channel, based on the crystal structures.
111 Furthermore, the trans-side funnel of the hourglass-shaped space is occupied at the exterior side by a short
112 α -helix, called a plug, between TM1 and TM2, resulting in a completely sealed SecY channel. Although
113 previous structural studies on the Sec translocon revealed that the cytoplasmic funnel of SecY is not occupied,
114 Tanaka et al. reported a high-resolution structure of SecYEG wherein the cytoplasmic loop of SecG covers
115 the cytoplasmic side of the channel²⁷, thus restricting membrane permeability in a manner similar to that of
116 the plug domain (Fig. 2D). Therefore, the SecG loop can function as a cytoplasmic cap for the SecY channel.
117 The cytoplasmic N-terminal region of Sec β is disordered in structural models; however, it could be located
118 near the cytoplasmic funnel in the resting state, similar to the SecG loop. The mechanism underlying this
119 covering process from each side of the pore ring may be universally conserved. The boundary area between
120 TM1–5 and TM6–10 of SecY on the opposite side of the tilted SecE transmembrane α -helix is called a lateral
121 gate, comprising TM2, 3, 7, and 8, which are binding sites for the signal sequences³³. The Sec translocon in
122 the resting states is not wide enough for protein transport. Therefore, the pore ring, plug, cap, and lateral gate
123 regions have been predicted to undergo conformational changes and/or are dislocated, thereby enabling
124 protein translocation across and integration into the membrane via the Sec translocon. The variable models of
125 the Sec translocon have been experimentally verified^{27,34-37}. Recent structural X-ray crystallographic^{21,23-28},
126 electron microscopic³⁸⁻⁴⁴, and functional^{45,46} analyses strongly suggested that the oligomeric state of the Sec
127 translocon is one heterotrimeric unit, although an efficient functional state comprising two or more units
128 cannot be excluded^{47,48}. Several crystal structures of the SecY complex imply that interactions between SecA,
129 Fab, or a peptide mimicking a part of the signal peptide and the protruded cytoplasmic regions of SecY
130 (which are intrinsically flexible) induce conformational changes in the lateral gate (Fig. 2E). Similar to these
131 crystal structures, binding of cytosolic factors to the Sec translocon would trigger structural changes to easily
132 interact with precursor proteins initially during protein translocation. In the SecA-bound conformation of
133 SecY, the plug domain is dislocated outwards, thereby expanding the inner space of SecY. This structural
134 change may lower the energy barrier to protein translocation via SecY.

135

136 Sec translocon in the protein translocation state

137 An outstanding report shows the crystal structure of SecYE and precursor segment-inserted SecA at
138 3.7-Å resolution (Fig. 3A, B)²⁶. For the structural analysis, the polypeptide was artificially introduced into a
139 loop of SecA as a fusion protein, accompanied by the generation of an intermolecular disulfide bond between
140 the peptide and SecY at the trans side of the plasma membrane to stabilize the protein-translocation
141 intermediate. The lateral gate is the most widely open in the available crystal structures. The signal peptide of
142 the substrate is located at the expanded lateral gate, surrounded by TM2, 3, and 7, presumably oriented
143 toward the hydrophobic regions of the lipid bilayer. During insertion, the signal peptide can be laterally
144 released from the expanded gate to the membrane via hydrophobic interactions. The part of the substrate
145 being transported is located along the center of the Sec translocon, and the pore ring is larger than that in
146 other crystal structures. Four of six residues of the pore were found to tightly interact with the transported
147 peptide, simultaneously blocking membrane permeability like a gasket. Hence, even during protein
148 translocation, SecY can maintain the membrane barrier simultaneously.

149

150 Recent structural studies of Sec translocon

151 Recent structural studies on the ribosome–Sec translocon complex by electron microscopy at medium
152 resolution revealed densities corresponding to the α -helices and conformational changes in transmembrane
153 regions and the localization of precursor proteins, providing insights into protein translocation across and
154 integration into the membrane³⁸⁻⁴⁴. Furthermore, samples can be directly observed by electron microscopy
155 without crystallization steps, which are needed for X-ray crystallography. Electron microscopic images of the
156 ribosome–nascent chain complex (RNC) probably include various intermediate states of SecY complexes,
157 thus providing several snapshots of co-translational translocation. The cryo-electron microscopic structure of
158 Sec61 and RNC, including a signal peptide, elucidated that the signal peptide is observed in a manner similar
159 to that of the SecYE–SecA–signal peptide complex (Fig. 3C, left)⁴². A different cryo-electron microscopic
160 imaging analysis of SecY and RNC, including two newly synthesized transmembrane α -helices, revealed that
161 two transmembrane regions are peripherally located near the lateral gate of SecY (Fig. 3C, right)³⁸. This

162 structure is considered to represent the intermediate state after the substrate is sorted into the membrane via
163 the Sec translocon. Although the electron density of the translocating peptide was unclear upon electron
164 microscopic analyses, probably owing to its unfolded conformation, polypeptides are thought to traverse the
165 central pore of the Sec translocon. Cryo-electron microscopic analysis has revealed several snapshots of the
166 active Sec translocon during protein translocation. Because the Sec translocon contains highly motile regions,
167 including the plug, cap, and cytoplasmic regions, we cannot accurately refine the structural models of the Sec
168 translocon at atomic resolution using the current electron density data at limited resolution, thus preventing
169 an accurate understanding of the transition states of the Sec translocon. Future structural analyses are required
170 at a higher resolution. Highly flexible regions may not be visible even in high-resolution structures
171 determined by X-ray crystallography, but cryo-electron microscopic analysis may elucidate several forms of
172 such flexible regions because recently developed programs can analyze several states separately. Structural
173 studies of the Sec translocon have indicated that the passive Sec translocon has a flexible structure, which
174 appropriately changes to direct the transportation of proteins to the trans side of the plasma membrane or into
175 the membrane, in response to interactions with cytosolic factors and precursor proteins. The fundamental
176 concepts underlying transitions of the Sec translocon (including changes in pore size, opening and closing the
177 lateral gate, and plug dislocation) were reported with the first crystal structure of the Sec translocon²¹ and
178 have been supported by structure-based functional studies for more than a decade¹.

179

180 **Overall structures of YidC**

181 The YidC core comprises five conserved transmembrane α -helices (cTM1–5) (Fig. 1C). The
182 arrangements of the transmembrane α -helices of YidC were predicted based on an evolutionary co-variation
183 analysis⁴⁹; however, the detailed interactions, arrangements, and tilting angles of the transmembrane regions
184 remain unknown. Crystal structures of YidC derived from three species were published (Table 1) in the past
185 five years⁵⁰⁻⁵³. All reported crystal structures for YidC displayed monomeric states (Fig. 4A–C), concurrent
186 with recent functional and structural reports that YidC functions as a monomer⁵⁴⁻⁵⁶, although functional
187 dimeric states of YidC have been previously proposed^{57,58}. The first transmembrane α -helix (1st TM) of *E.*

188 *coli* YidC, which functions as a signal sequence, was disordered even in the recent higher-resolution crystal
189 structure (Fig. 4A)⁵⁰. Furthermore, the 1st TM was reported to interact with SecY and SecE⁵⁹ and to be
190 involved in substrate binding^{60,61}; however, the significance of this interaction is not yet clear. The first
191 periplasmic regions (P1) of *E. coli* and *T. maritima* (Fig. 1C) do not share the same architecture, suggesting
192 that the P1 region is not essential in *E. coli*⁶². However, a part of the P1 region of *E. coli* interacts with Sec
193 components and YidC^{63,64}, potentially contributing to the formation of the Sec holo-translocon complex⁶⁵. The
194 N-terminal extension of cTM1, called EH1, is a conserved amphiphilic helix parallel to the membrane surface.
195 The hydrophobic half of EH1 is embedded in the membrane. EH1 may function as a float to stabilize YidC
196 localization in the membrane. The five conserved transmembrane α -helices create a hydrophilic cavity (Fig.
197 4B). A comparison of the transmembrane regions of the reported crystal structures of YidC revealed that
198 hydrophilic cavities of the same size are evolutionarily conserved among YidC family proteins (Fig. 4D).

199

200 **Detailed structures and functions of YidC**

201 The cavity is positively charged and exposed to the cytoplasm and the membrane, whereas the
202 trans side of the plasma membrane is entirely closed by tightly packed hydrophobic residues (Fig. 4B). At the
203 center of the cavity, a conserved positively charged residue, Arg, in *B. halodurans*, *T. maritima*, and *E. coli*,
204 primarily contributes to the characterized positive charge of the cavity (Fig. 4C). The positive charge in *B.*
205 *halodurans* was shown to be essential for cell growth and insertion of MifM, a substrate of YidC⁵¹. In
206 contrast, the positive charge in *E. coli* is important, but replaceable^{52,66}. The difference in positive charge
207 requirements may be related to the importance of the functions of substrate proteins of YidC in each species.
208 Systematic mutational analysis revealed that the hydrophilicity of this region is also an important factor
209 influencing YidC activity⁶⁷. Short, rigid loops of the trans side, showing lower B-factors upon
210 crystallographic analysis, structurally support the closed extracellular side of the transmembrane region. On
211 the opposite side, the C1 loop forms a hairpin loop comprising two hydrophilic α -helices, which protrude
212 from the transmembrane region to the cytoplasm. It has been suggested that the C1 region contains sites for
213 interaction with substrates⁵⁹. The arrangements of the C1 regions in the crystal structures are not the same, i.e.,

214 they are flexible, concurrent with higher B-factors in the C1 region compared to other core regions (Fig. 4E).
215 In the case of *T. maritima* YidC, the cytoplasmic loops, including the C1 loop, were disordered. Although the
216 C2 loop was disordered in reported crystal structure models (except for the structure reported most recently),
217 the 2.8-Å resolution data from *E. coli* YidC helped characterize the C2 loop (Fig. 4C, E). The C2 loop is
218 located near the entrance of the hydrophilic cavity. The B-factors of the C2 loop are even higher than those of
219 the C1 loop, implying that the C2 region is most flexible in the core of YidC. The C2 loop at the cavity
220 entrance may function as a cover to prevent excessive exposure of hydrophilic regions in the membrane. The
221 fundamental role of C2 may be similar to that of the SecE loop²⁷. The crystal structure of *B. halodurans* YidC
222 (Form II) (Fig. 4C, right) only shows the C-terminal region, which interacts with the C1 region. Because the
223 C-terminal, C1, and C2 regions were reported to interact with the ribosome^{54,68,69}, the cytoplasmic regions
224 may bind the ribosome cooperatively. Functional analysis using deletion mutations supported the importance
225 of the loops of the core region⁵¹. Because YidC contains a hydrophilic cavity facing the membrane interior,
226 YidC may preferably not exist stably in the hydrophobic membrane. Three molecular dynamics simulations
227 of YidC revealed that YidC can stably exist in the membrane with some cytoplasmic fluctuations^{50,51,70}.
228 During the simulations, the cavity of YidC was filled with approximately 20 water molecules. One of the
229 important functions of the transmembrane region of YidC is to generate a pool of water molecules at the
230 membrane. Together, the structure derived from all conserved regions from EH1 to cTM5 seem crucial for
231 YidC activity. The conserved, positively charged cavity of YidC could reflect the importance of electrostatic
232 interactions. A certain type of YidC substrate is negatively charged. In the case of the
233 single-membrane-spanning substrate MifM, three positively charged residues are positioned at the N-terminal
234 region. When the negatively charged residues were mutated, the MifM-insertion activity of YidC decreased,
235 thus increasing the possibility that the interaction between the positive charge in the hydrophilic cavity and
236 the negative charges of substrates is important for YidC-dependent membrane protein insertion⁵¹.
237 Subsequently, a site-specific photo-crosslinking analysis elucidated direct interactions between the cavity and
238 MifM⁵¹. Hence, a membrane-insertion model of a simple membrane protein such as a once-spanning or
239 twice-spanning transmembrane protein resulting from YidC activity has been proposed (Fig. 5A). Initially

240 during protein insertion by YidC, the flexible C1 and C2 regions may recognize and interact with the
241 substrate, and then the substrate is temporally captured by the YidC cavity, which is mediated by electrostatic
242 and hydrophilic interactions between the substrate and YidC. Thereafter, the captured substrate protein is
243 sorted from the cavity into the membrane via hydrophobic interactions with membrane lipids. The
244 non-uniform distribution of electrostatic charges resulting from the membrane potential derived from the
245 proton motive force further influences protein sorting.

246

247 **Conserved mechanism of membrane protein insertion**

248 Cryo-electron microscopic analysis of the RNC and YidC complex showed the transmembrane
249 segments of a substrate in the front of the entrance of the cavity exposed to the membrane⁴⁹. This state is
250 assumed to be adopted immediately after the substrate is released from the YidC cavity. A
251 molecular-dynamics simulation suggested that the thickness of the membrane surrounding YidC was reduced
252 by the existence of YidC, thus decreasing the local energy barrier of protein translation across the
253 membrane⁷⁰. A similar reduction in thickness was previously reported based on a molecular-dynamics
254 simulation of the outer-membrane protein BamA⁷¹, which functions as a membrane protein insertase for the
255 outer membrane. Owing to the lack of energy sources such as ATP at the outer membrane, protein insertion is
256 achieved via a delicate balance involving molecular interactions, collision frequency, and concentration.
257 YidC-like proteins identified in Archaea and in the ER membrane of eukaryotes contain three transmembrane
258 α -helices, corresponding to cTM1, 2, and 5 in YidC, which are proposed to form a hydrophilic surface similar
259 to that of YidC^{72,73}. The functional roles of YidC family proteins and the YidC-like proteins may be conserved
260 in each membrane as primitive machinery.

261

262 **Collaborative functional model of SecYEG and YidC for membrane protein insertion**

263 YidC functions not only as an insertase, but also as a membrane chaperone for integrating certain
264 types of multi-membrane-spanning proteins into the membrane in collaboration with SecYEG^{74,75}.
265 Cross-linking experiments revealed that cTM3 and cTM5 mainly interact with substrates^{60,76}, and the lateral

266 gate of SecY interacts with YidC⁶⁴. Therefore, the entrance for the lipid bilayer of YidC should face the lateral
267 gate of SecYEG. To elucidate the molecular mechanism underlying collaborative protein integration, the
268 detailed three-dimensional structure of the complex of YidC and SecYEG warrants elucidation. Based on the
269 cryo-electron microscopic structure of the Sec holo-translocon complex at ~10-Å resolution⁷⁷, it is difficult to
270 discuss the detailed interactions and conformational transitions of the components. Further high-resolution
271 structural analysis studies are required. The cryo-electron microscopic structures of RNC in complex with
272 SecYEG or YidC have been reported previously, as described above. Therefore, future studies may
273 potentially reveal the structure of the RNC–YidC–SecYEG complex at improved resolution. As the
274 hydrophilic cavity of YidC faces the membrane, YidC can shelter the hydrophilic region of the newly
275 synthesized membrane protein being sorted from the lateral gate of the Sec translocon. The number of YidC
276 molecules in the cell would be greater than that of SecYEG⁷⁸, presumably enabling several YidCs to function
277 simultaneously as chaperones for Sec-dependent membrane integration/maturation, which is important for
278 membrane protein biogenesis. The mechanism underlying substrate recognition by YidC as a chaperone
279 during membrane protein folding is in complete contrast with that of soluble chaperones, which typically
280 provide hydrophobic surfaces to prevent misfolding of soluble proteins (Fig. 4B). The positively charged
281 YidC cavity preferentially interacts with and transports negatively charged regions of substrates to the
282 opposite side, such that YidC is more likely to be involved in the positive inside rule of membrane proteins⁷⁹.
283 Several YidC substrates have been identified¹⁷; however, identification of other YidC substrates is necessary
284 to further clarify the details regarding YidC-mediated capture and release of substrates into the membrane.
285 Unidentified substrates with high stability even in an aqueous buffer are preferable for functional analysis,
286 especially for in vitro experiments with purified proteins.

287

288 **Concluding remarks**

289 Considering recent developments in electron microscopy, crystallization procedures, and data-collection
290 systems, determination of high-resolution structures as snapshots during protein translocation is promising. In
291 high-resolution cryo-electron microscopic structural analyses of the Sec translocon and YidC in

292 co-translational translocation studies, the samples contained ribosomes, the size of which allowed the
293 construction of molecular models. In contrast, X-ray crystallography is considered desirable for structural
294 analysis in post-translational translocation studies, because the Sec translocon complex lacks a ribosome.
295 However, the latest structural studies of the post-translational *Saccharomyces cerevisiae* Sec61 complex
296 (consisting of Sec61 $\alpha/\gamma/\beta$, Sec62/63, and Sec71/72) by cryo-electron microscopy and single-particle analysis
297 was reported at a maximum resolution of 3.4 Å⁸⁰ and 4.1 Å⁸¹. It is noteworthy that the authors built molecular
298 models of Sec translocon without a ribosome structure. Similar to that of SecY in Fig. 2E, the lateral gate of
299 Sec61 is opened by cytosolic interactions. In addition, a Sec61 β –Sec63 fusion protein was used for the
300 former⁸⁰ study to stabilize the post-translational Sec translocon complex. A bacterial SecY–SecA fusion
301 protein, possessing protein-translocation activity, can be embedded into nanodisc particles⁸². Therefore,
302 further structural analysis of the Sec translocon in the post-translational pathway, without a ribosome, can be
303 performed by electron microscopy in combination with some fusion proteins to uncover several detailed
304 intermediate architectures. In the near future, electron microscopy will be considered one of the more
305 powerful tools for structural analysis at atomic resolution, even for post-translational protein translocation
306 studies. Moreover, time-dependent structural analyses are also required to further the current understanding of
307 protein transport. Single-molecule analysis helps resolve the underlying mechanism^{83,84}, and high-speed
308 atomic force microscopic observations of one unit may provide an overall view of structural changes
309 occurring during protein translocation in real time⁸⁵. Numerous interesting questions regarding a
310 comprehensive understanding of protein transport remain to be answered.

311

312 **ACKNOWLEDGMENTS**

313 I thank K. Abe for providing secretarial assistance. This review was supported by the JSPS/MEXT
314 KAKENHI (grant numbers JP26119007, JP18H02405, and JP18KK0197).

315

316 **Table 1 | Crystal structures of the Sec translocon and YidC**

Species	Resolution	States	Notes	PDB ID	Reference
Sec translocon					
<i>Methanocaldococcus jannaschii</i> SecYE β	3.2 Å	Resting state	Stable mutant	1RH5	21
	3.5 Å	Resting state		1RHZ	21
	3.5 Å		Plug mutant	2YXQ	28
	3.6 Å		Plug mutant	2YXR	28
<i>Thermus thermophilus</i> SecYE + Fab	3.2 Å	Fab-bound		2ZJS	23
<i>Thermotoga maritima</i> SecYEG + SecA	4.5 Å	SecA-bound		3DIN	25
<i>Pyrococcus furiosus</i> SecYE	2.9 Å	C-terminal interacting		3MP7	24
<i>Thermus thermophilus</i> SecYEG	2.7 Å	Resting state	Best resolution	5AWW	27
	3.6 Å	Peptide-bound		5CH4	27
<i>Geobacillus thermodenitrificans</i> SecYE + SecA + nanobody	3.7 Å	Precursor-bound	SecA-precursor fusion	5EUL	26
YidC					
<i>Bacillus halodurans</i> YidC	2.4 Å	Form I		3WO6	51
	3.2 Å	Form II		3WO7	51
<i>Escherichia coli</i> YidC	3.2 Å			3WVF	52
	2.8 Å		All YidC cores modeled	6AL2	50
<i>Thermotoga maritima</i> YidC	3.8 Å			5Y83	53

317

318

319 **Figure legends**320 **Figure 1 | Bacterial protein translocation and integration via the Sec translocon and YidC.**

321 A, Protein translocation across and integration into the membrane. During post-translational translocation,
322 precursor proteins with an N-terminal signal sequence are targeted to and translocated across the membrane,
323 which is driven by Sec62/63 complex and BiP in eukaryotes and SecA ATPase and SecDF in bacteria. During
324 co-translational translocation, the ribosome–nascent chain complex (RNC) is directed to the membrane by the
325 interaction between signal recognition particle (SRP) and its receptor, and interacts with SecYEG or YidC.
326 Subsequent membrane protein integration via the interior of the Sec translocon and/or YidC occurs
327 co-translationally. B, Schematic representation of Sec translocon components. C, Schematic representation of
328 the YidC/Oxa1/Alb3 protein family.

329

330 **Figure 2 | Crystal structures of the Sec translocon.**

331 A, The Sec translocon in the resting state. Crystal structures of SecYE β from *Methanocaldococcus jannaschii*
332 (PDB ID 1RH5) (left) and SecYEG from *Thermus thermophilus* (PDB ID 5AWW) (right). B, Schematic
333 representation of the Sec translocon. C, Magnified views of the pore ring of the structures in A from the
334 cytoplasm. D, Cut-away models of the surface representation of *T. thermophilus* SecYEG without the plug
335 and cap regions. The plug and cap regions are represented by the ribbon model with a stick model for the side
336 chains. E, Crystal structures of the Sec translocons in which the cytoplasmic region interacts with other
337 molecules in the crystals (PDB ID 3MP7, 5CH4, 2ZJS, and 3DIN).

338

339 **Figure 3 | Structures of the Sec translocon in the intermediate stages of protein transport.**

340 A, Crystal structures of the SecYEG–SecA complex with part of the precursor protein expressed as a fusion
341 protein (PDB ID 5EUL). B, Magnified views of the pore ring of the structure in A from the cytoplasmic side .
342 C, Electron microscopic structures of the Sec translocon of the RNC complex during protein transport (PDB
343 ID 3JC2 and 5ABB).

344

345 **Figure 4 | Crystal structures of YidC.**

346 A, Crystal structure of *E. coli* YidC at 2.8-Å resolution, elucidating all YidC core regions (PDB ID 6AL2).
347 The cTM numbers are shown. B, Cut-away model of the *E. coli* YidC structure. C, Gallery of crystal
348 structures of YidC (PDB ID 6AL2, 5Y83, 3WO6, and 3WO7). D, Superimposition of the core region of *B.*
349 *halodurans*, *T. maritima*, and *E. coli* YidCs. E, Magnified view of the C1 loop region.

350

351 **Figure 5 | Functional model of YidC.**

352 A, Membrane-insertion model of a single-membrane-spanning protein via YidC, independently of SecYEG.
353 YidC temporally captures the precursor protein at the positively charged cavity. Thereafter, the substrate
354 protein is sorted primarily via hydrophobic interactions. B, Chaperone activity model of YidC. YidC protects
355 a hydrophilic region sorted from the lateral gate of the Sec translocon until its interacting region emerges
356 from the gate, promoting correct folding of substrate proteins.

357

358 **References**

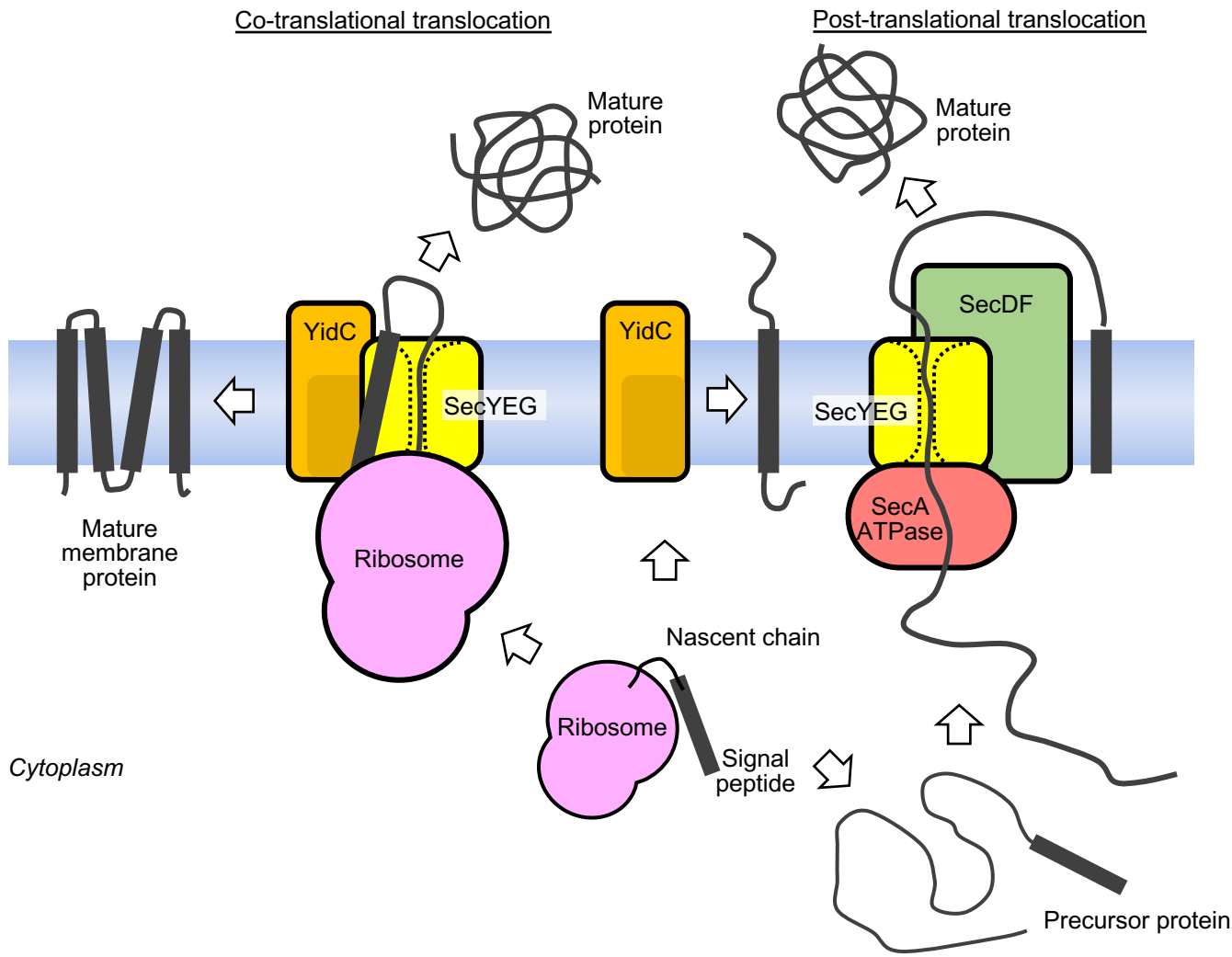
- 359
- 360 1 Rapoport, T. A., Li, L. & Park, E. Structural and Mechanistic Insights into Protein Translocation. *Annu Rev Cell*
- 361 *Dev Biol*, doi:10.1146/annurev-cellbio-100616-060439 (2017).
- 362 2 Tsirigotaki, A., De Geyter, J., Sostaric, N., Economou, A. & Karamanou, S. Protein export through the bacterial
- 363 Sec pathway. *Nat Rev Microbiol* **15**, 21-36, doi:10.1038/nrmicro.2016.161 (2017).
- 364 3 Blobel, G. & Dobberstein, B. Transfer of proteins across membranes. *J Cell Biol* **67**, 835-862 (1975).
- 365 4 Akopian, D., Shen, K., Zhang, X. & Shan, S. O. Signal recognition particle: an essential protein-targeting
- 366 machine. *Annu Rev Biochem* **82**, 693-721, doi:10.1146/annurev-biochem-072711-164732 (2013).
- 367 5 Matlack, K. E., Misselwitz, B., Plath, K. & Rapoport, T. A. BiP acts as a molecular ratchet during
- 368 posttranslational transport of prepro-alpha factor across the ER membrane. *Cell* **97**, 553-564 (1999).
- 369 6 Chatzi, K. E., Sardis, M. F., Economou, A. & Karamanou, S. SecA-mediated targeting and translocation of
- 370 secretory proteins. *Biochim Biophys Acta* **1843**, 1466-1474, doi:10.1016/j.bbamcr.2014.02.014 (2014).
- 371 7 Hartl, F. U., Lecker, S., Schiebel, E., Hendrick, J. P. & Wickner, W. The binding cascade of SecB to SecA to
- 372 SecY/E mediates preprotein targeting to the E. coli plasma membrane. *Cell* **63**, 269-279 (1990).
- 373 8 Economou, A. & Wickner, W. SecA promotes preprotein translocation by undergoing ATP-driven cycles of
- 374 membrane insertion and deinsertion. *Cell* **78**, 835-843 (1994).
- 375 9 Braunger, K. *et al.* Structural basis for coupling protein transport and N-glycosylation at the mammalian
- 376 endoplasmic reticulum. *Science*, doi:10.1126/science.aar7899 (2018).
- 377 10 Pfeffer, S. *et al.* Dissecting the molecular organization of the translocon-associated protein complex. *Nat*
- 378 *Commun* **8**, 14516, doi:10.1038/ncomms14516 (2017).
- 379 11 Tsukazaki, T. Structure-based working model of SecDF, a proton-driven bacterial protein translocation factor.
- 380 *FEMS Microbiol Lett* **365**, doi:10.1093/femsle/fny112 (2018).
- 381 12 Duong, F. & Wickner, W. Distinct catalytic roles of the SecYE, SecG and SecDFyajC subunits of preprotein
- 382 translocase holoenzyme. *Embo J* **16**, 2756-2768 (1997).
- 383 13 Tsukazaki, T. *et al.* Structure and function of a membrane component SecDF that enhances protein export.
- 384 *Nature* **474**, 235-238, doi:10.1038/nature09980 (2011).
- 385 14 Furukawa, A., Nakayama, S., Yoshikaie, K., Tanaka, Y. & Tsukazaki, T. Remote Coupled Drastic beta-Barrel to
- 386 beta-Sheet Transition of the Protein Translocation Motor. *Structure* **26**, 485-489 e482,
- 387 doi:10.1016/j.str.2018.01.002 (2018).
- 388 15 Furukawa, A. *et al.* Tunnel Formation Inferred from the I-Form Structures of the Proton-Driven Protein
- 389 Secretion Motor SecDF. *Cell Rep* **19**, 895-901, doi:10.1016/j.celrep.2017.04.030 (2017).
- 390 16 Kiefer, D. & Kuhn, A. YidC-mediated membrane insertion. *FEMS Microbiol Lett* **365**,
- 391 doi:10.1093/femsle/fny106 (2018).
- 392 17 Hennon, S. W., Soman, R., Zhu, L. & Dalbey, R. E. YidC/Oxa1/Alb3 Family of Insertases. *J Biol Chem* **290**,
- 393 14866-14874, doi:10.1074/jbc.R115.638171 (2015).
- 394 18 Nishikawa, H., Sasaki, M. & Nishiyama, K. I. Membrane insertion of F0 c subunit of F0F1 ATPase depends on
- 395 glycolipoyzyme MPase and is stimulated by YidC. *Biochem Biophys Res Commun* **487**, 477-482,
- 396 doi:10.1016/j.bbrc.2017.04.095 (2017).
- 397 19 Nishiyama, K. *et al.* MPase is a glycolipoyzyme essential for membrane protein integration. *Nat Commun* **3**,
- 398 1260, doi:10.1038/ncomms2267 (2012).
- 399 20 Wang, P. & Dalbey, R. E. Inserting membrane proteins: the YidC/Oxa1/Alb3 machinery in bacteria,
- 400 mitochondria, and chloroplasts. *Biochim Biophys Acta* **1808**, 866-875, doi:10.1016/j.bbamem.2010.08.014
- 401 (2011).
- 402 21 van den Berg, B. *et al.* X-ray structure of a protein-conducting channel. *Nature* **427**, 36-44,
- 403 doi:10.1038/nature02218 (2004).
- 404 22 du Plessis, D. J., Nouwen, N. & Driessen, A. J. The Sec translocase. *Biochim. Biophys. Acta* **1808**, 851-865,
- 405 doi:10.1016/j.bbamem.2010.08.016 (2011).
- 406 23 Tsukazaki, T. *et al.* Conformational transition of Sec machinery inferred from bacterial SecYE structures.
- 407 *Nature* **455**, 988-991 (2008).
- 408 24 Egea, P. F. & Stroud, R. M. Lateral opening of a translocon upon entry of protein suggests the mechanism of
- 409 insertion into membranes. *Proc Natl Acad Sci USA* **107**, 17182-17187, doi:10.1073/pnas.1012556107 (2010).
- 410 25 Zimmer, J., Nam, Y. & Rapoport, T. A. Structure of a complex of the ATPase SecA and the protein-translocation
- 411 channel. *Nature* **455**, 936-943, doi: 10.1038/nature07335 (2008).
- 412 26 Li, L. *et al.* Crystal structure of a substrate-engaged SecY protein-translocation channel. *Nature* **531**, 395-399,
- 413 doi:10.1038/nature17163 (2016).
- 414 27 Tanaka, Y. *et al.* Crystal Structures of SecYEG in Lipidic Cubic Phase Elucidate a Precise Resting and a

- 415 Peptide-Bound State. *Cell Rep* **13**, 1561-1568, doi:10.1016/j.celrep.2015.10.025 (2015).
- 416 28 Li, W. *et al.* The plug domain of the SecY protein stabilizes the closed state of the translocation channel and
417 maintains a membrane seal. *Mol Cell* **26**, 511-521 (2007).
- 418 29 Flower, A. M., Hines, L. L. & Pfennig, P. L. SecG is an auxiliary component of the protein export apparatus of
419 Escherichia coli. *Mol Gen Genet* **263**, 131-136 (2000).
- 420 30 Nishiyama, K., Hanada, M. & Tokuda, H. Disruption of the gene encoding p12 (SecG) reveals the direct
421 involvement and important function of SecG in the protein translocation of Escherichia coli at low temperature.
422 *EMBO J* **13**, 3272-3277 (1994).
- 423 31 Bost, S. & Belin, D. A new genetic selection identifies essential residues in SecG, a component of the
424 Escherichia coli protein export machinery. *Embo J* **14**, 4412-4421 (1995).
- 425 32 Brundage, L., Hendrick, J. P., Schiebel, E., Driessen, A. J. & Wickner, W. The purified E. coli integral
426 membrane protein SecY/E is sufficient for reconstitution of SecA-dependent precursor protein translocation.
427 *Cell* **62**, 649-657 (1990).
- 428 33 Plath, K., Mothes, W., Wilkinson, B. M., Stirling, C. J. & Rapoport, T. A. Signal sequence recognition in
429 posttranslational protein transport across the yeast ER membrane. *Cell* **94**, 795-807 (1998).
- 430 34 Tam, P. C., Maillard, A. P., Chan, K. K. & Duong, F. Investigating the SecY plug movement at the SecYEG
431 translocation channel. *EMBO J* **24**, 3380-3388 (2005).
- 432 35 Allen, W. J. *et al.* Two-way communication between SecY and SecA suggests a Brownian ratchet mechanism
433 for protein translocation. *elife* **5**, doi:10.7554/eLife.15598 (2016).
- 434 36 Cannon, K. S., Or, E., Clemons, W. M., Jr., Shibata, Y. & Rapoport, T. A. Disulfide bridge formation between
435 SecY and a translocating polypeptide localizes the translocation pore to the center of SecY. *J Cell Biol* **169**,
436 219-225 (2005).
- 437 37 Ge, Y., Draycheva, A., Bornemann, T., Rodnina, M. V. & Wintermeyer, W. Lateral opening of the bacterial
438 translocon on ribosome binding and signal peptide insertion. *Nat Commun* **5**, 5263, doi:10.1038/ncomms6263
439 (2014).
- 440 38 Bischoff, L., Wickles, S., Berninghausen, O., van der Sluis, E. O. & Beckmann, R. Visualization of a polytopic
441 membrane protein during SecY-mediated membrane insertion. *Nat Commun* **5**, 4103, doi:10.1038/ncomms5103
442 (2014).
- 443 39 Gogala, M. *et al.* Structures of the Sec61 complex engaged in nascent peptide translocation or membrane
444 insertion. *Nature* **506**, 107-110, doi:10.1038/nature12950 (2014).
- 445 40 Park, E. *et al.* Structure of the SecY channel during initiation of protein translocation. *Nature* **506**, 102-106,
446 doi:10.1038/nature12720 (2014).
- 447 41 Voorhees, R. M., Fernandez, I. S., Scheres, S. H. & Hegde, R. S. Structure of the mammalian ribosome-Sec61
448 complex to 3.4 Å resolution. *Cell* **157**, 1632-1643, doi:10.1016/j.cell.2014.05.024 (2014).
- 449 42 Voorhees, R. M. & Hegde, R. S. Structure of the Sec61 channel opened by a signal sequence. *Science* **351**,
450 88-91, doi:10.1126/science.aad4992 (2016).
- 451 43 Pfeffer, S. *et al.* Structure of the native Sec61 protein-conducting channel. *Nat Commun* **6**, 8403,
452 doi:10.1038/ncomms9403 (2015).
- 453 44 Jomaa, A., Boehringer, D., Leibundgut, M. & Ban, N. Structures of the E. coli translating ribosome with SRP
454 and its receptor and with the translocon. *Nat Commun* **7**, 10471, doi:10.1038/ncomms10471 (2016).
- 455 45 Kedrov, A., Kusters, I., Krasnikov, V. V. & Driessen, A. J. A single copy of SecYEG is sufficient for preprotein
456 translocation. *The EMBO journal* **30**, 4387-4397, doi:10.1038/emboj.2011.314 (2011).
- 457 46 Park, E. & Rapoport, T. A. Bacterial protein translocation requires only one copy of the SecY complex in vivo.
458 *J Cell Biol* **198**, 881-893, doi:10.1083/jcb.201205140 (2012).
- 459 47 Dalal, K., Chan, C. S., Sligar, S. G. & Duong, F. Two copies of the SecY channel and acidic lipids are necessary
460 to activate the SecA translocation ATPase. *Proceedings of the National Academy of Sciences of the United*
461 *States of America* **109**, 4104-4109, doi:10.1073/pnas.1117783109 (2012).
- 462 48 Osborne, A. R. & Rapoport, T. A. Protein translocation is mediated by oligomers of the SecY complex with one
463 SecY copy forming the channel. *Cell* **129**, 97-110 (2007).
- 464 49 Kedrov, A. *et al.* Structural Dynamics of the YidC:Ribosome Complex during Membrane Protein Biogenesis.
465 *Cell Rep* **17**, 2943-2954, doi:10.1016/j.celrep.2016.11.059 (2016).
- 466 50 Tanaka, Y. *et al.* 2.8-Å crystal structure of Escherichia coli YidC revealing all core regions, including flexible
467 C2 loop. *Biochem Biophys Res Commun* **505**, 141-145, doi:10.1016/j.bbrc.2018.09.043 (2018).
- 468 51 Kumazaki, K. *et al.* Structural basis of Sec-independent membrane protein insertion by YidC. *Nature* **509**,
469 516-520, doi:10.1038/nature13167 (2014).
- 470 52 Kumazaki, K. *et al.* Crystal structure of Escherichia coli YidC, a membrane protein chaperone and insertase. *Sci*
471 *Rep* **4**, 7299, doi:10.1038/srep07299 (2014).

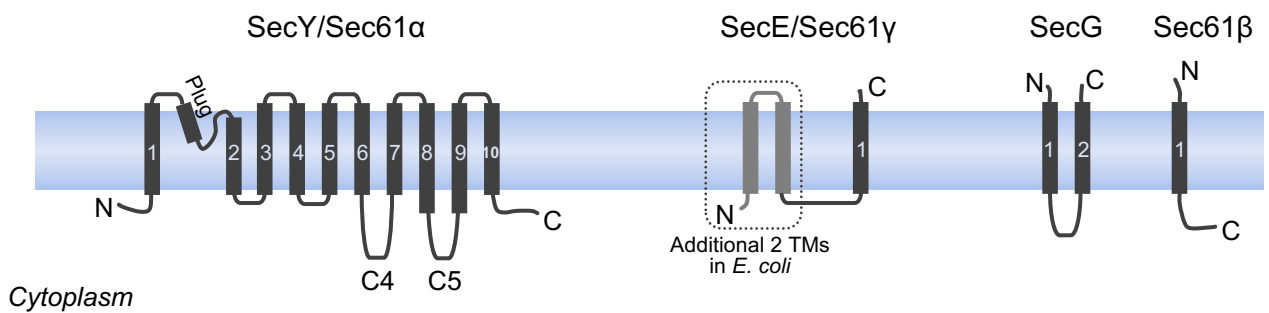
- 472 53 Xin, Y. *et al.* Structure of YidC from *Thermotoga maritima* and its implications for YidC-mediated membrane
473 protein insertion. *FASEB J* **32**, 2411-2421, doi:10.1096/fj.201700893RR (2018).
- 474 54 Kedrov, A. *et al.* Elucidating the native architecture of the YidC: ribosome complex. *J Mol Biol* **425**, 4112-4124,
475 doi:10.1016/j.jmb.2013.07.042 (2013).
- 476 55 Wickles, S. *et al.* A structural model of the active ribosome-bound membrane protein insertase YidC. *elife* **3**,
477 e03035, doi:10.7554/eLife.03035 (2014).
- 478 56 Spann, D., Pross, E., Chen, Y., Dalbey, R. E. & Kuhn, A. Each protomer of a dimeric YidC functions as a single
479 membrane insertase. *Sci Rep* **8**, 589, doi:10.1038/s41598-017-18830-9 (2018).
- 480 57 Kohler, R. *et al.* YidC and Oxal form dimeric insertion pores on the translating ribosome. *Mol Cell* **34**, 344-353,
481 doi:10.1016/j.molcel.2009.04.019 (2009).
- 482 58 Lotz, M., Haase, W., Kuhlbrandt, W. & Collinson, I. Projection structure of yidC: a conserved mediator of
483 membrane protein assembly. *J Mol Biol* **375**, 901-907, doi:10.1016/j.jmb.2007.10.089 (2008).
- 484 59 Petriman, N. A. *et al.* The interaction network of the YidC insertase with the SecYEG translocon, SRP and the
485 SRP receptor FtsY. *Sci Rep* **8**, 578, doi:10.1038/s41598-017-19019-w (2018).
- 486 60 Klenner, C. & Kuhn, A. Dynamic disulfide scanning of the membrane-inserting Pf3 coat protein reveals
487 multiple YidC substrate contacts. *J Biol Chem* **287**, 3769-3776, doi:10.1074/jbc.M111.307223 (2012).
- 488 61 Klenner, C., Yuan, J., Dalbey, R. E. & Kuhn, A. The Pf3 coat protein contacts TM1 and TM3 of YidC during
489 membrane biogenesis. *FEBS Lett* **582**, 3967-3972, doi:10.1016/j.febslet.2008.10.044 (2008).
- 490 62 Jiang, F. *et al.* Defining the regions of *Escherichia coli* YidC that contribute to activity. *J Biol Chem* **278**,
491 48965-48972 (2003).
- 492 63 Xie, K., Kiefer, D., Nagler, G., Dalbey, R. E. & Kuhn, A. Different regions of the nonconserved large
493 periplasmic domain of *Escherichia coli* YidC are involved in the SecF interaction and membrane insertase
494 activity. *Biochemistry* **45**, 13401-13408 (2006).
- 495 64 Sachelar, I. *et al.* YidC occupies the lateral gate of the SecYEG translocon and is sequentially displaced by a
496 nascent membrane protein. *J Biol Chem* **288**, 16295-16307, doi:10.1074/jbc.M112.446583 (2013).
- 497 65 Schulze, R. J. *et al.* Membrane protein insertion and proton-motive-force-dependent secretion through the
498 bacterial holo-translocon SecYEG-SecDF-YajC-YidC. *Proc Natl Acad Sci U S A* **111**, 4844-4849,
499 doi:10.1073/pnas.1315901111 (2014).
- 500 66 Chen, Y., Soman, R., Shanmugam, S. K., Kuhn, A. & Dalbey, R. E. The role of the strictly conserved positively
501 charged residue differs among the Gram-positive, Gram-negative, and chloroplast YidC homologs. *J Biol Chem*
502 **289**, 35656-35667, doi:10.1074/jbc.M114.595082 (2014).
- 503 67 Shimokawa-Chiba, N. *et al.* Hydrophilic microenvironment required for the channel-independent insertase
504 function of YidC protein. *Proc Natl Acad Sci U S A* **112**, 5063-5068, doi:10.1073/pnas.1423817112 (2015).
- 505 68 Geng, Y. *et al.* Role of the Cytosolic Loop C2 and the C Terminus of YidC in Ribosome Binding and Insertion
506 Activity. *J Biol Chem* **290**, 17250-17261, doi:10.1074/jbc.M115.650309 (2015).
- 507 69 Seitz, I., Wickles, S., Beckmann, R., Kuhn, A. & Kiefer, D. The C-terminal regions of YidC from
508 *Rhodospirillum rubrum* and *Oceanicaulis alexandrii* bind to ribosomes and partially substitute for SRP receptor
509 function in *Escherichia coli*. *Mol Microbiol* **91**, 408-421, doi:10.1111/mmi.12465 (2014).
- 510 70 Chen, Y. *et al.* YidC Insertase of *Escherichia coli*: Water Accessibility and Membrane Shaping. *Structure* **25**,
511 1403-1414 e1403, doi:10.1016/j.str.2017.07.008 (2017).
- 512 71 Noinaj, N. *et al.* Structural insight into the biogenesis of beta-barrel membrane proteins. *Nature* **501**, 385-390,
513 doi:10.1038/nature12521 (2013).
- 514 72 Anghel, S. A., McGilvray, P. T., Hegde, R. S. & Keenan, R. J. Identification of Oxal Homologs Operating in
515 the Eukaryotic Endoplasmic Reticulum. *Cell Rep* **21**, 3708-3716, doi:10.1016/j.celrep.2017.12.006 (2017).
- 516 73 Borowska, M. T., Dominik, P. K., Anghel, S. A., Kossiakoff, A. A. & Keenan, R. J. A YidC-like Protein in the
517 Archaeal Plasma Membrane. *Structure* **23**, 1715-1724, doi:10.1016/j.str.2015.06.025 (2015).
- 518 74 Nagamori, S., Smirnova, I. N. & Kaback, H. R. Role of YidC in folding of polytopic membrane proteins. *J Cell*
519 *Biol* **165**, 53-62, doi:10.1083/jcb.200402067 (2004).
- 520 75 Serdiuk, T. *et al.* YidC assists the stepwise and stochastic folding of membrane proteins. *Nat Chem Biol* **12**,
521 911-917, doi:10.1038/nchembio.2169 (2016).
- 522 76 Yu, Z., Konigstein, G., Pop, A. & Lührink, J. The conserved third transmembrane segment of YidC contacts
523 nascent *Escherichia coli* inner membrane proteins. *J Biol Chem* **283**, 34635-34642,
524 doi:10.1074/jbc.M804344200 (2008).
- 525 77 Botte, M. *et al.* A central cavity within the holo-translocon suggests a mechanism for membrane protein
526 insertion. *Sci Rep* **6**, 38399, doi:10.1038/srep38399 (2016).
- 527 78 Urbanus, M. L. *et al.* Targeting, insertion, and localization of *Escherichia coli* YidC. *J Biol Chem* **277**,
528 12718-12723 (2002).

- 529 79 von Heijne, G. The distribution of positively charged residues in bacterial inner membrane proteins correlates
530 with the trans-membrane topology. *EMBO J* **5**, 3021-3027 (1986).
- 531 80 Itskanov, S. & Park, E. Structure of the posttranslational Sec protein-translocation channel complex from yeast.
532 *Science*, doi:10.1126/science.aav6740 (2018).
- 533 81 Wu, X., Cabanos, C. & Rapoport, T. A. Structure of the post-translational protein translocation machinery of
534 the ER membrane. *Nature* **566**, 136-139, doi:10.1038/s41586-018-0856-x (2019).
- 535 82 Sugano, Y., Furukawa, A., Nureki, O., Tanaka, Y. & Tsukazaki, T. SecY-SecA fusion protein retains the ability
536 to mediate protein transport. *PLoS One* **12**, e0183434, doi:10.1371/journal.pone.0183434 (2017).
- 537 83 Kedrov, A., Kusters, I. & Driessen, A. J. Single-molecule studies of bacterial protein translocation.
538 *Biochemistry* **52**, 6740-6754, doi:10.1021/bi400913x (2013).
- 539 84 Taufik, I., Kedrov, A., Exterkate, M. & Driessen, A. J. Monitoring the activity of single translocons. *J Mol Biol*
540 **425**, 4145-4153, doi:10.1016/j.jmb.2013.08.012 (2013).
- 541 85 Haruyama, T. *et al.* Single-Unit Imaging of Membrane Protein-Embedded Nanodiscs from Two Oriented Sides
542 by High-Speed Atomic Force Microscopy. *Structure*, doi:10.1016/j.str.2018.09.005 (2018).
- 543

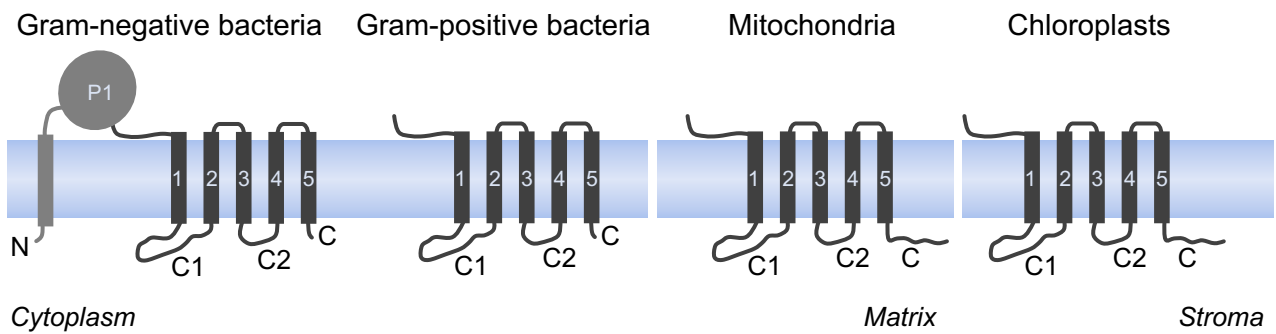
A Bacterial protein translocation



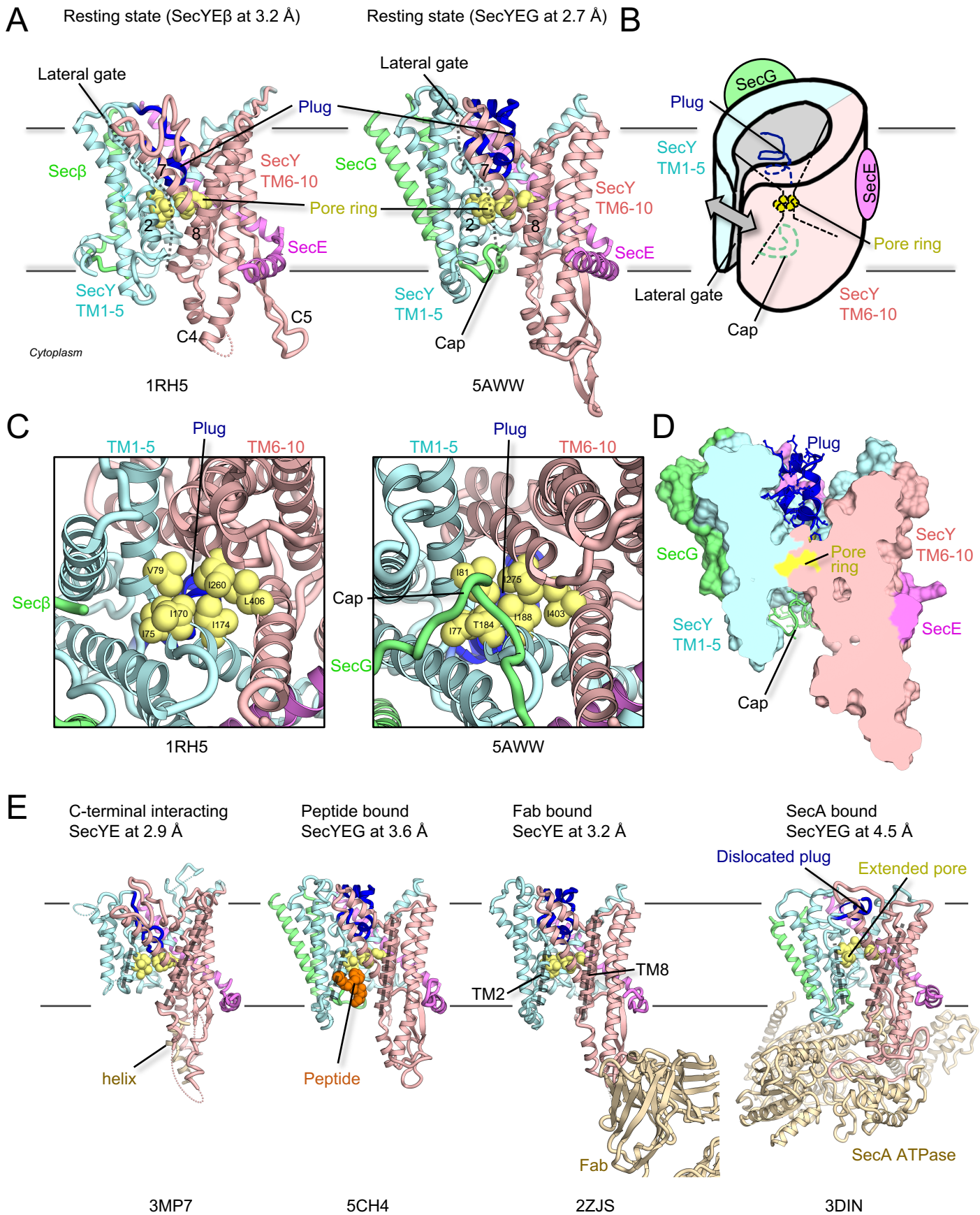
B Sec translocon components



C YidC/Oxa1/Alb3 family

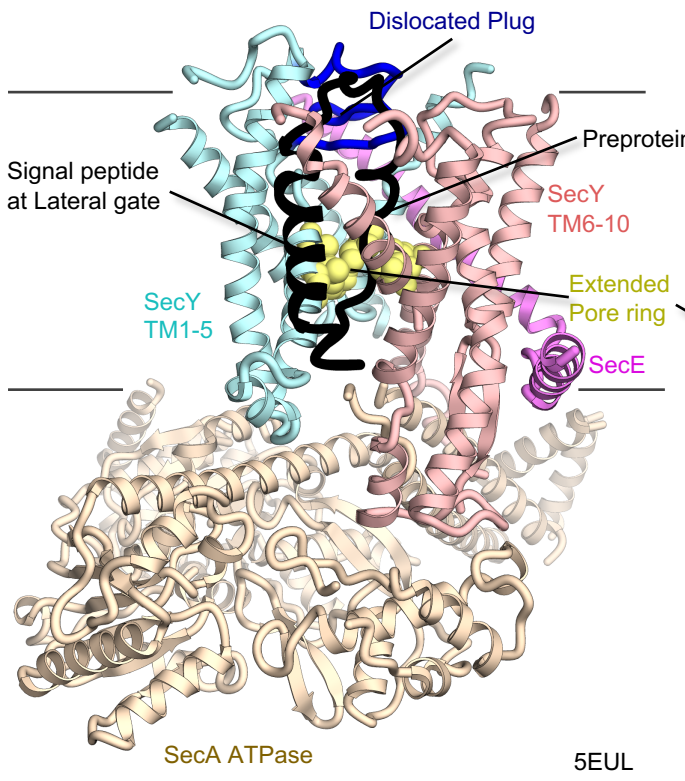


Tsukazaki Fig. 1

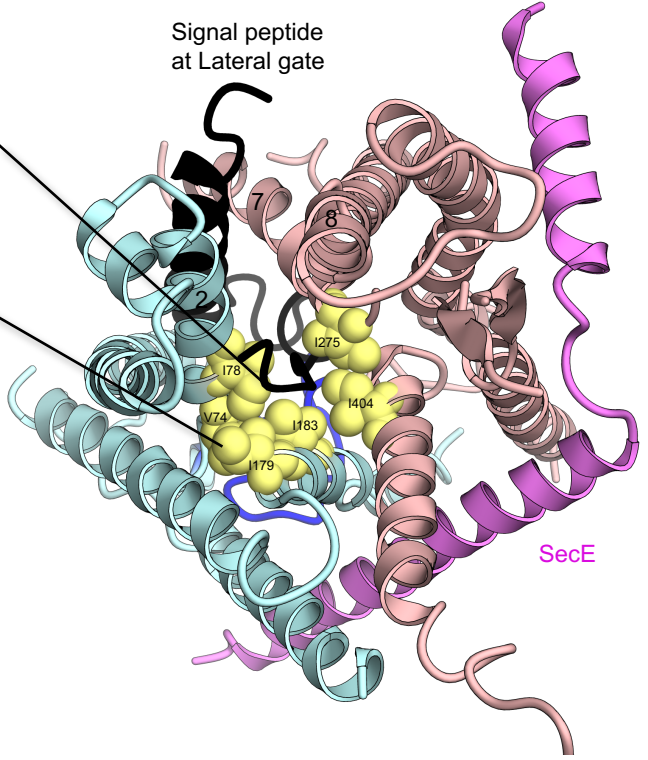


Tsukazaki Fig. 2

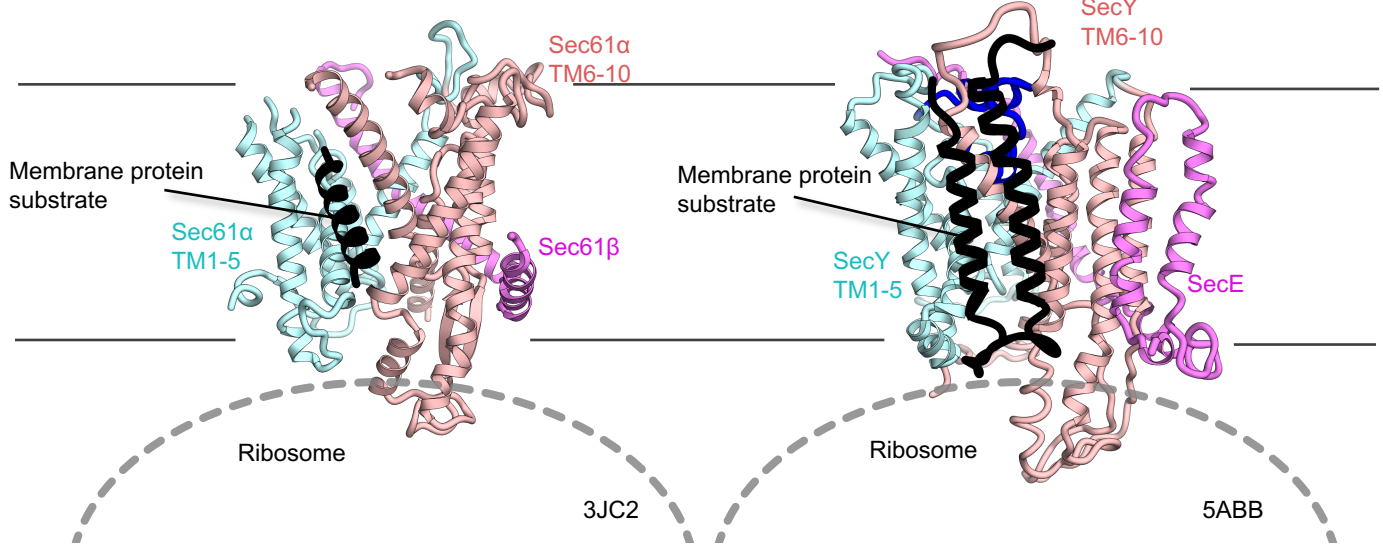
A Protein translocation intermediate states
SecYE-SecA at 3.7 Å

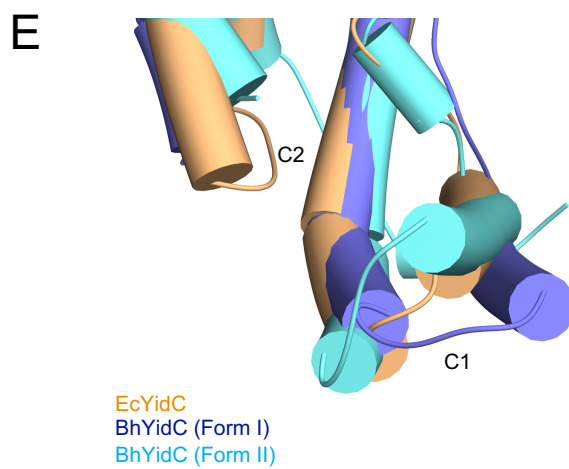
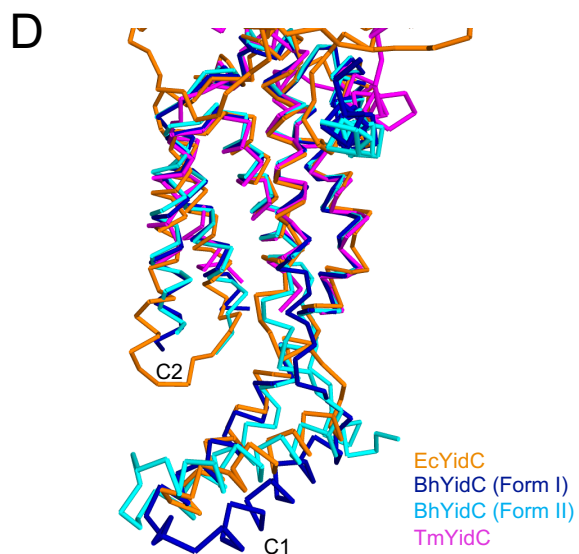
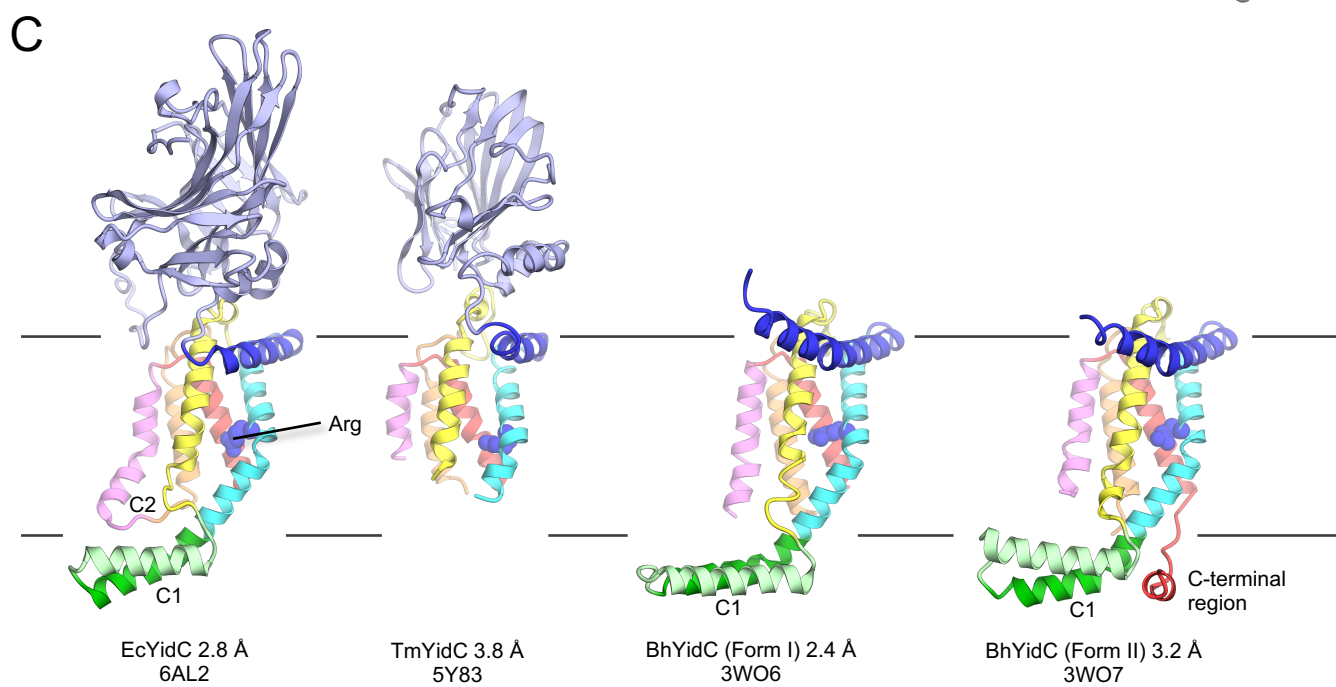
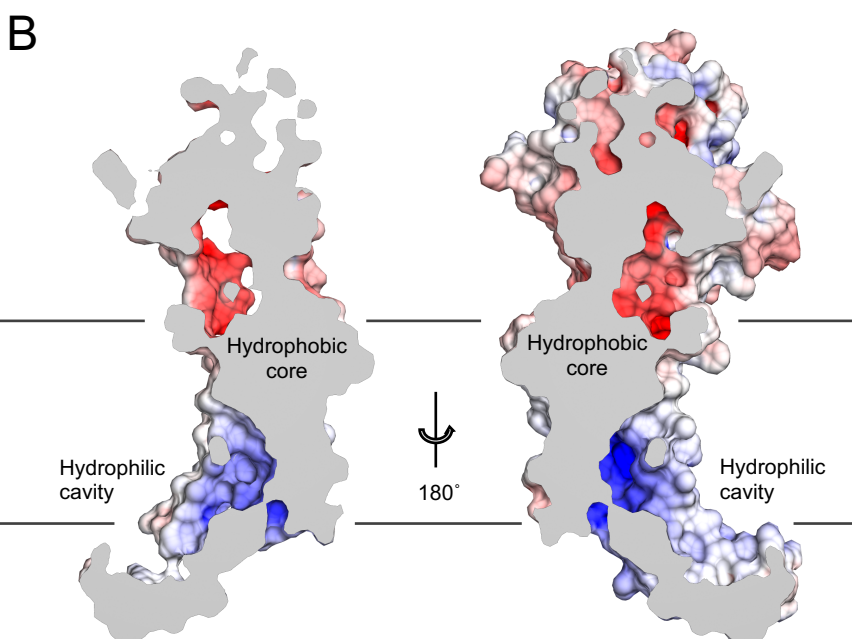
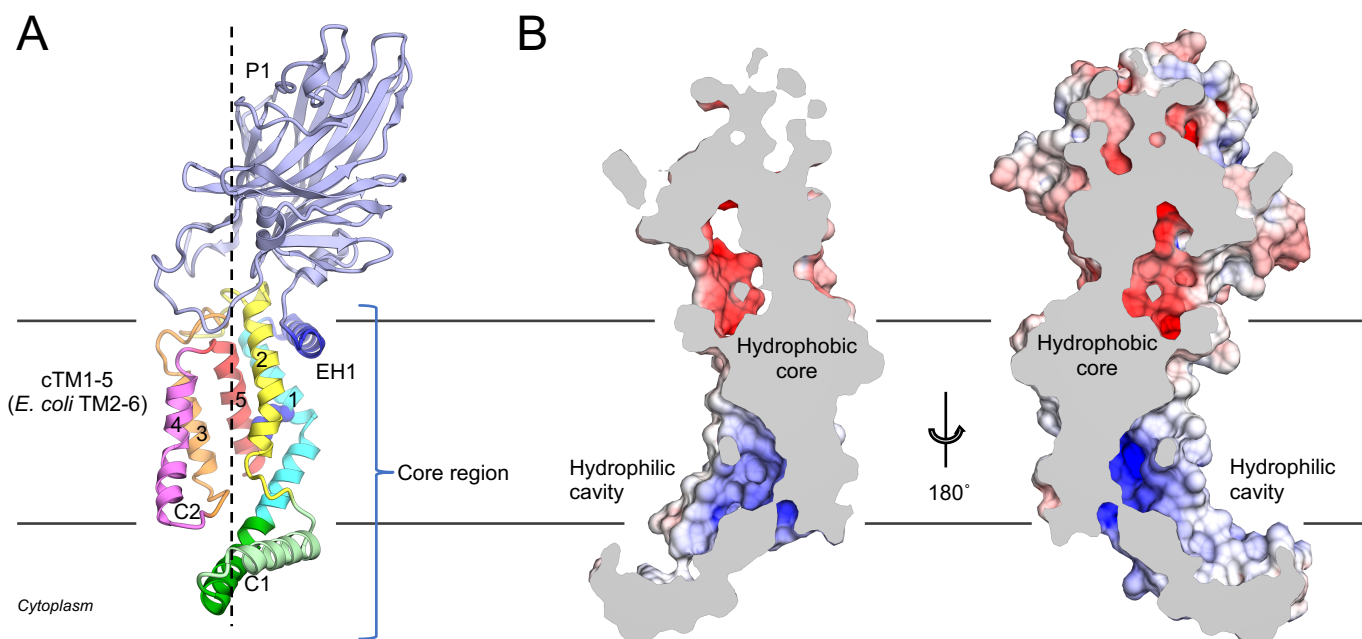


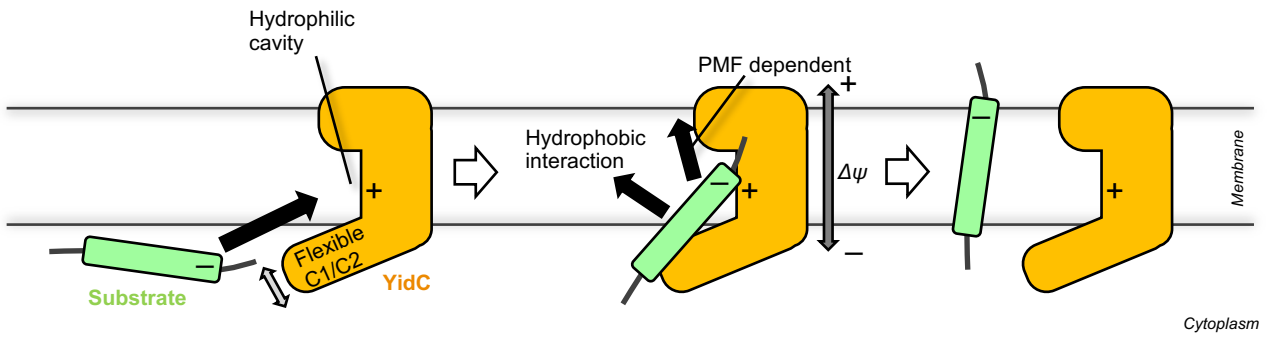
B



C EM structures of co-translational translocation





A**B**